

Multiple electronic components and Lifshitz transitions by oxygen wires formation in layered cuprates and nickelates

Thomas Jarlborg^{1,2} and Antonio Bianconi^{2,3,4}

¹*DQMP, University of Geneva, 24 Quai Ernest-Ansermet, CH-1211 Geneva 4, Switzerland*

²*RICMASS Rome International Center for Materials Science Superstripes, Via dei Sabelli 119A, 00185 Rome, Italy*

³*Institute of Crystallography, Consiglio Nazionale delle Ricerche, CNR, Monterotondo, Roma, I-00015, Italy*

⁴*National Research Nuclear University MEPhI (Moscow Engineering Physics Institute), 115409 Moscow, Russia*

There is a growing compelling experimental evidence that a quantum complex matter scenario made of multiple electronic components, and competing quantum phases is needed to grab the key physics of high critical temperature (T_c) superconductivity in layered cuprates. While it is known that defects self-organization controls T_c , the mechanism remains an open issue. Here we focus on the theoretical prediction of the multi-band electronic structure and the formation of broken Fermi surfaces generated by the self-organization of oxygen interstitials O_i atomic wires in the spacer layers in $\text{HgBa}_2\text{CuO}_{4+y}$, $\text{La}_2\text{CuO}_{4\pm\delta}$ and $\text{La}_2\text{NiO}_{4\pm\delta}$, by means of self-consistent Linear Muffin-Tin Orbital (LMTO) calculations. The electronic structure of a first phase of ordered O_i atomic wires and of a second glassy phase made of disordered O_i impurities have been studied through supercell calculations. We show the common features of the influence of O_i wires in the electronic structure in three type of materials. The ordering of O_i into wires lead to a separation of the electronic states between the O_i ensemble and the rest of the bulk. The wires formation produce first quantum confined localized states near the wire which coexist with second delocalized states in the Fermi-surface (FS) of doped cuprates. In this new scenario for high T_c superconductivity, Kitaev wires with Majorana bound states are proximity-coupled to a 2D d-wave superconductor in cuprates.

PACS numbers: 74.20.Pq, 74.72.-h, 74.25.Jb

I. INTRODUCTION.

The mechanism behind the emergence of high T_c superconductivity remains object of high scientific interest [1–3]. All high T_c superconductors show a superconducting dome, centered at the maximum T_{Cmax} tuning the chemical potential by doping or pressure. The high T_c superconductivity violates the standard approximations of BCS theory [4]: 1) the *dirty limit* approximation reducing the electronic structure to a single effective Fermi surface and 2) the *Migdal* approximation where chemical potential is far away from band edges. Considering a rigid lattice and neglecting electronic correlations the density-of-states (DOS) at the Fermi energy (E_F) in cuprates is not high, which is in sharp contrast to what standard BCS theory of superconductivity would suggest. The exchange of Cu with Ni permits a much higher DOS at E_F without major changes of the lattice, but the nickelates are not superconducting.

The popular theoretical paradigms assuming a rigid tetragonal structure for the CuO_2 plane and a single electronic component model have been abandoned. The multiband complexity arising from the competition between the effects of multiple orbitals in dopant induced $3d^9L(a_1)$ and $3d^9L(b_1)$ electronic states in the Mott Hubbard charge transfer gap [5, 6], misfit strain [7, 8], incommensurate lattice modulations [9], spin density waves, charge density waves [10], and dopants nanoscale organization [10, 11] need to be clarified to understand the quantum complex matter scenario made of multiple interacting complex networks [12, 13].

Recently the consensus is growing on the proposal that

the high T_c superconducting dome [14] in cuprates is confined between topological Lifshitz transitions [15] for the appearing of new spots of Fermi surfaces [9, 16, 17]. typical of multiband superconductors [18, 19] and it is predicted by the solution of Bogoliubov equations in the stripes scenario. The electronic structure is strongly modified by stripes pattern formation with formation of Fermi arcs. determined either by 1D short range polaronic Wigner charge density waves and lattice effects as lattice tilts typical of perovskites under strain and bond disproportionation associated with the $3d^9L$ states induced by doping and the self-organization of oxygen interstitials and defects are expected to contribute to the topological Lifshitz transitions in the quantum complex matter scenario of high temperature superconductors.

The experimental fact that the critical temperature T_c in cuprates appears be controlled by interstitials and defects self organization [20–22] has motivated us to study the electronic structures of large supercells of some cuprates and nickelates containing ordered atomic 'wires' of oxygen ions on interstitial positions.

The systems that we have considered here are $\text{La}_2\text{CuO}_{4\pm\delta}$ (LCO) [23], $\text{La}_2\text{NiO}_{4\pm\delta}$ (LNO) [24], and $\text{HgBa}_2\text{CuO}_{4+y}$ (Hg1201) [25]. Self-consistent Linear Muffin-Tin Orbital (LMTO) band calculations for supercells of different sizes have been made for the structures with and without oxygen interstitial (O_i) impurities. The total DOS in the three systems near E_F show large, seemingly chaotic, peaks, as the number of O_i are added, even if they are ordered in "wires". However, by comparing the Fermi surfaces (FS) in the Brillouin Zone (BZ) for the elementary cell and the supercells for the cuprate

systems we concluded that most of the normal FS of the CuO_2 layers remain intact despite the additions of ordered impurities. The large DOS peaks are localized on the impurities with little spillover to nearest neighbors. A long-range charge transfer of electrons from the CuO (and NiO) layers on the the O_i -wires (p-doping) will modify the size of the typical FS cylinder in the case of cuprates. In this paper we review some of the results and add some complimentary information in order to get a global picture of wire formation in these systems.

Defect self-organization has been found to control the critical temperature in $\text{Sr}_2\text{CuO}_{4-y}$ [30], in $\text{Sr}_{2-x}\text{Ba}_x\text{CuO}_{3+y}$ [31], in $(\text{Cu}_{0.75}\text{Mo}_{0.25}\text{Sr}_2\text{YCu}_2\text{O}_{7+y})$ with $0 < y < 0.5$ [32, 33], and in $\text{BaPb}_{1-x}\text{Bi}_x\text{O}_3$ [34]. The oxygen interstitial organization in oxygen doped cuprates $\text{La}_2\text{CuO}_{4+y}$ has been studied by scanning micro x-ray diffraction [11, 20, 21, 35–39], and by STM [40–42] showing superconductivity emerging in a nanoscale phase separation with a complex geometry [43–47] which is determined by the proximity to a electronic topological Lifshitz transition in strongly correlated electronic systems [48–50]. In fact it has been found that the domes of high critical temperature occurs by tuning the chemical potential near topological Lifshitz transitions in many different cuprates [19, 51–54] including the case of pressurized sulfur hydride [1–3].

A considerable theoretical work has shown how the electronic states near the Fermi level respond to the lattice and dopants organization changing the topology of the Fermi surface [23–25, 55–60]. The interest is focused to the perspective that a the quasi one-dimensional ordering of dopants could generate stripes giving a quasi 1D electronic structure at the Fermi level. The new periodicity driven by oxygen interstitial self organization sets up a potential modulation, which generates unconventional topological Lifshitz transition for the appearing of new bands.

Doping is crucial for high- T_c superconductivity. It is usually controlled by the exchange of the heavy atoms with different valency, like Sr (or Ba) for La in $\text{La}_{2-x}\text{Sr}_x\text{CuO}_4$. But varying the O-occupation has also been proven to be efficient for doping, either as a vacancy or as an interstitial impurity. The Fermi surface for doping larger than 0.21 holes per Cu sites is expected to be predicted by band structure calculations. Superconductivity can be enhanced by ordering of oxygen interstitials in cuprates like $\text{La}_2\text{CuO}_{4+\delta}$ [21]. Band calculations show that oxygen vacancies in the apical positions in $\text{Ba}_2\text{CuO}_{4-\delta}$ (BCO, with $\delta \approx 1$) make its electronic structure very similar to that of optimally doped La_2CuO_4 (LCO) [56, 57]. The T_c of BCO is reported to be much larger than in LCO [31]. Self organization of oxygen interstitials enhances T_c [21], and the Fermi surface (FS) can become fragmented by oxygen self organization [23]. However, the exact role of *ordering* of the defects is not well known in many cases. Recently experimental results have been reported on self organization of oxygen interstitials in doped cuprates

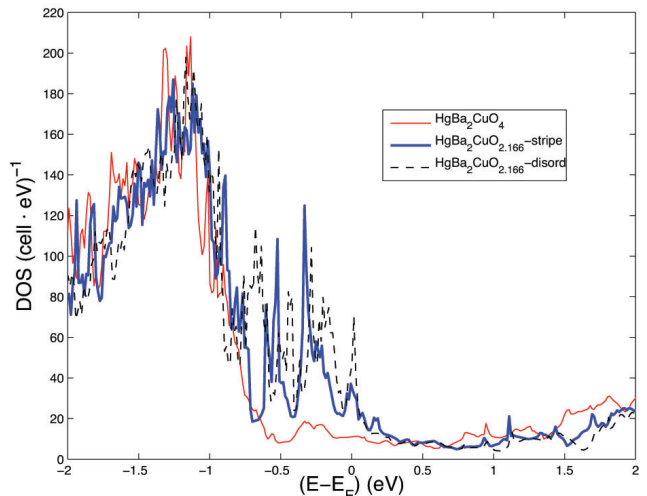


FIG. 1: (Color online) The total DOS for $\text{Hg}_{12}\text{Ba}_2\text{Cu}_{12}\text{O}_{48+N}$ with $N=0$ (thin red) and $N=2$ (bold blue). The (black) broken line is when the two O atoms occupy sites far from each other (“disordered”).

$\text{HgBa}_2\text{CuO}_{4+y}$ [10, 12]. by scanning micro x-ray diffraction which provide complementary information on local nanoscale structure investigation using x-ray absorption spectroscopy [61–63] using EXAFS and XANES methods [64, 65] which probe the deviation of the local structure from the average structure. In this work we discuss electronic structure results for the hole-doped oxygen-enriched $\text{HgBa}_2\text{CuO}_{4.167}$, ($\text{Hg}1201$), $\text{La}_2\text{CuO}_{4+\delta}$ (LCO) and $\text{La}_2\text{NiO}_{4+\delta}$ (LNO). The method of calculation is presented in sect. II, in sect. III we discuss the results, and conclusions are in sect. IV.

II. METHOD OF CALCULATION.

The calculations are made using the linear muffin-tin orbital (LMTO) method [66, 67] and the local spin-density approximation (LSDA) [68, 69]. The details of the methods have been published earlier [23–25, 60, 70, 71, 75].

The supercell $\text{Hg}_{12}\text{Ba}_{24}\text{Cu}_{12}\text{O}_{48+2}$ is extended 6- and 2-lattice constants along x and y , respectively. The 2 additional oxygens are inserted in the Hg-plane, as is known to be the position of excess O in HBCO. These oxygens form a stripe running along y .

Calculations for the elementary cell of HBCO need 8 atomic sites and 5 “empty spheres”, which are included in the most open part of the structure, see ref. [70]. The empty sphere in the Hg plane, at $(0.5, 0.5, 0)$, is the location of excess oxygen. The lattice constant a_0 is 3.87 Å, and $c/a=2.445$. The elementary cell is extended $6a_0$ along x and $2a_0$ along y . The empty spheres at $(0.5, 0.5, 0)$ and $(0.5, 1.5, 0)$, and at $(0.5, 0.5, 0)$ and $(2.5, 1.5, 0)$ are occupied by O in the “stripe” supercell and “disordered” supercells, respectively. This is in the latter case the most

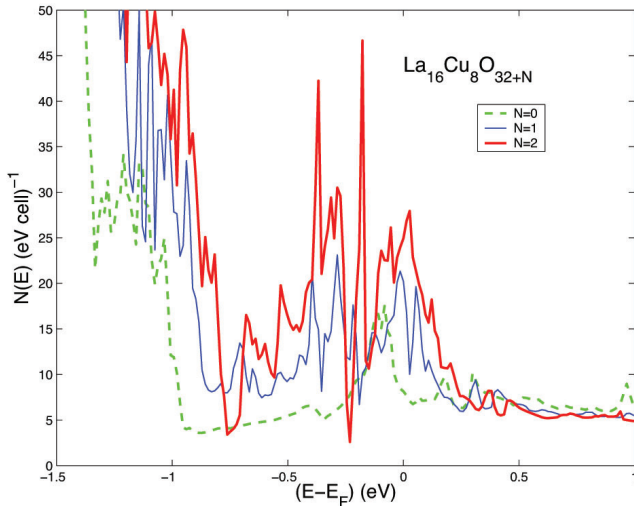


FIG. 2: (Color online) The total DOS for $\text{La}_{16}\text{Cu}_8\text{O}_{32+N}$ with $N=0, 1$ and 2 near E_F . The Cu-d band edge moves upwards with increasing N , which is an effect of p-doping. Large DOS peaks near E_F are localized at the O_i impurities. The O_i -wire for $N=2$ becomes electronically isolated from the rest of the p-doped cuprate system, but this cannot be seen from the DOS functions.

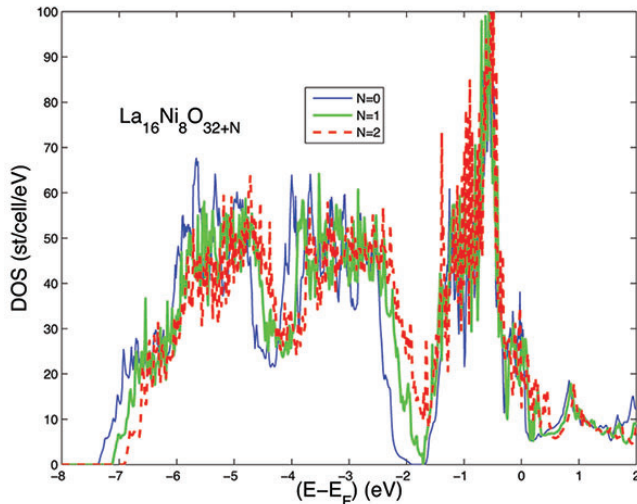


FIG. 3: (Color online) The total DOS for $\text{La}_{16}\text{Ni}_8\text{O}_{32+N}$ with $N=0, 1$ and 2 . The number of fully occupied O-p bands in the range -7 to -2 eV increases with increasing N . Nevertheless, a weak effective p-doping can be detected by the Ni-d band edge as it moves through E_F for increasing N .

distant and uncorrelated choice for the two interstitial O impurities.

The elementary cell of La_2NiO_4 (LNO) contains La sites at $(0,0,\pm.721c)$, Ni at $(0,0,0)$, planar O's at $(0.5,0,0)$ and $(0,.5,0)$ and apical O's at $(0,0,\pm.366c)$, in units of the lattice constant $a_0=3.86 \text{ \AA}$, where $c=1.16$. In addition to the MT-spheres at the atomic sites we insert MT-spheres at positions $(.5,0,\pm.5c)$ and $(0,.5,\pm.5c)$ to account for the

positions of empty spheres. The NIO supercells consist of six- and eight-fold repetition of the elementary cell along the plane axis.

In La_2CuO_4 (LCO) the sites are at the corresponding positions, but with the lattice constant $a = 3.8 \text{ \AA}$ and $c = 12.4 \text{ \AA}$. In addition to the MT spheres at the atomic sites we insert MT spheres at positions $(0.5,0,0.5c)$ and $(0,0.5,0.5c)$ to account for the positions of empty spheres. An elongated supercell is created by an eight-fold repetition of the elementary cell in the diagonal direction of the CuO_2 plane.

The doped cases are simulated in calculations where one or two empty interstitial sites have been replaced by O-i atoms. The total number of sites are different for the different calculations and with different total number of k-points. Information about this, the size of atomic spheres, basis set and so on can be found in the previous papers [23–25]. Note that our work is based on density functional theory (DFT) where correlation is a global function of the spin densities [68, 69]. Strong, non-DFT correlation is not expected for cuprates and nickelates with doping away from half-filling of the d-band. ARPES (angular-resolved photoemission spectroscopy) and ACAR (angular correlation of positron annihilation radiation) on cuprates have detected FS's and bands in agreement with DFT calculations [72–74]. Here we discuss mainly paramagnetic band results, but the calculations for LNO lead to ferromagnetic (FM) ground states, even though the FM moments decreases on Ni sites near to the O-i wires [24].

III. RESULTS.

The total DOS functions at the Fermi level for three supercells of the doped Hg-based cuprate are shown in Figs. 1. The undoped DOS agree with the DOS calculated previously for one unit cell of HBCO using also $\ell = 3$ states for the Ba sites [70]. A difference is that the less dense k-point mesh for the supercell makes the DOS curve less smooth. The total DOS at E_F per elementary cell is about $1.0 (\text{eV})^{-1}$ compared to 0.92 here for the supercell. A calculation of a supercell of intermediate size ($\text{Hg}_4\text{Ba}_8\text{Cu}_4\text{O}_{17}$) corresponding to an impurity concentration of 0.25 shows that the DOS at E_F increases by a factor of two to about 1.8 per elementary cell [59]. All atoms are close to the impurity in that case, which explains that the local peaks in the states are not so narrow as in the present case. Here E_F is on a narrow peak in both cells with O impurities, which makes the DOS higher, about 3 and $4 (\text{eV})^{-1}$ per elementary cell for the striped and disordered case respectively. The increase of the DOS is limited to the first layers of atoms adjacent to the impurity.

The addition of two ordered or disordered O_i in the cell makes new states to appear near E_F in the interval -0.6 to $+0.2$ eV, see Fig. 1. Therefore, it is not possible to judge about the effects of doping on the FS from these DOS

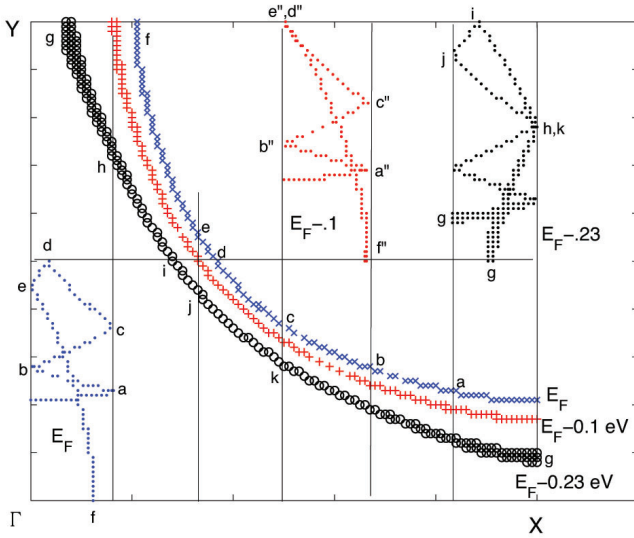


FIG. 4: (Color online) Upper large panel (Γ - X - Y) show the Fermi surface for one unitcell of undoped HBCO. The "x" is at the calculated E_F , the "+" for 0.1 eV down shifted, and "o" for 0.23 eV down shifted E_F . The small panels show how these FS look after folding the bands into the BZ for the 6×2 supercell.

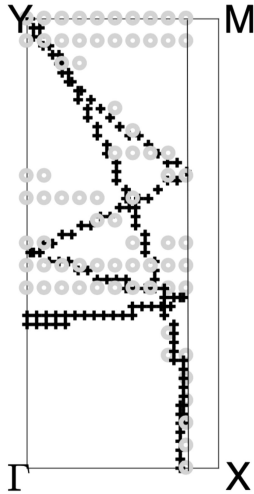


FIG. 5: (Color online) The FS of $\text{Hg}_{12}\text{Ba}_{24}\text{Cu}_{12}\text{O}_{48+N}$ for $N=2$ ('O-i wires', gray circles), and the folded FS for elementary HBCO with E_F down shifted 0.1 eV (black + signs), i.e. as in the small middle panel in Fig. 4. The two FS agree well, which show that the essentials of the FS-cylinder remain even when the O_2 -wire is present, but some p-type doping is present since E_F is reduced by 0.1 eV. The slight deviations for the bands crossing the $\Gamma - Y$ line can be understood from an unfolded supercell FS, in which the Fermi radius is shorter towards X , points a and b (cf. Fig. 4). The radius is also smaller than for undoped HBCO, while near points c, d and e the radius is larger and the agreement with undoped HBCO is good. However, there is a new band and a new FS at the top of the panel for the supercell. This band has a very high DOS on the O-i sites, and its FS cannot be explained by from the simple folding.

functions. However, it is possible to see that the d-band edge near -1 eV moves to the right, about 0.1 eV, when two ordered O_i have been added. This is an indication of an effective p-doping, i.e. equivalent of moving E_F to the left on the standard cuprate DOS. This finding is less evident for the disordered case. The evolution of the DOS with doping in LCO and LNO can be seen in Figs. 2 and 3.

In order to reveal the effect of doping on the FS we compare the FS of real calculation for the supercell with that of the folded FS of the simple FS as calculated for the single unit cell. The FS for one unit cell of HBCO is shown in Fig. 4. Three circular FS's are shown within one quarter of the BZ, all centered at the upper right corner of the BZ. One FS with the largest radius is for the calculated E_F , and two smaller FS are for assumed larger p-doping when E_F are 0.1 and 0.23 eV lower. Each of the smaller panels of Fig. 4 shows the extent of the BZ of the 6×2 supercell, and in three of them we show how the folded FS's would look like after folding. In the case of intermediate doping, shown by $E_F - 0.1$, one can note that the points marked as i and j in the FS at E_F (or e and d in the FS for $E_F - 0.23$) has merged into one point (marked by e'' and d''). This merged feature also appear in the FS calculated for the doped cell with ordered O_i , see Fig. 5. The folded FS for $E_F - 0.1$ (+ signs) agree well with the real FS for the supercell (o signs) almost coincides near the Y-point, which is an evidence of merged branches. Also at the X-point there is a good agreement, which is an indication of a FS with a radius close to what is indicated by f and f'' in Fig. 4 for the case $E_F - 0.1$. The FS structures for folded and real FS in the middle of Fig. 5 have the same shapes. This shows that a circular FS survives despite the doping of ordered O_i , but that the radius near point b in Fig. 4 should be a bit smaller, i.e the circle seems to slightly retract near this point.

Thus, there are convincing indications that the typical cuprate FS survives despite ordered O_i doping. However, on the upper edge of the BZ in Fig. 5 is seen a clear FS that cannot be understood from folding. A close look at the states making this FS branch shows that it consists of O_i -p states. The DOS is very high on O_i with only little spill over on to the nearest neighbors. Hybridization with the p-states on the oxygen impurity atoms makes fairly large s- and d-DOS on Hg, and an increase of the p-DOS on the nearest apical oxygen states, while the influence on planar O and Ba is not large. The Cu sites are quite distant from the O_i , and the Cu d-DOS increases about 35 percent near the impurity, and by 25 percent on the more distant Cu compared to the undoped case. This increased DOS on Cu is similar as the increased DOS that follows from p-doping, i.e. from a lowering of E_F when it is approaching the van-Hove DOS peak as in other cuprates. Again, this is a hint that p-type doping is a result of the addition of O_i . When the dopants are disordered we also expect some p-doping effect on the d-band edge (see above), but as is shown in ref. [25] the

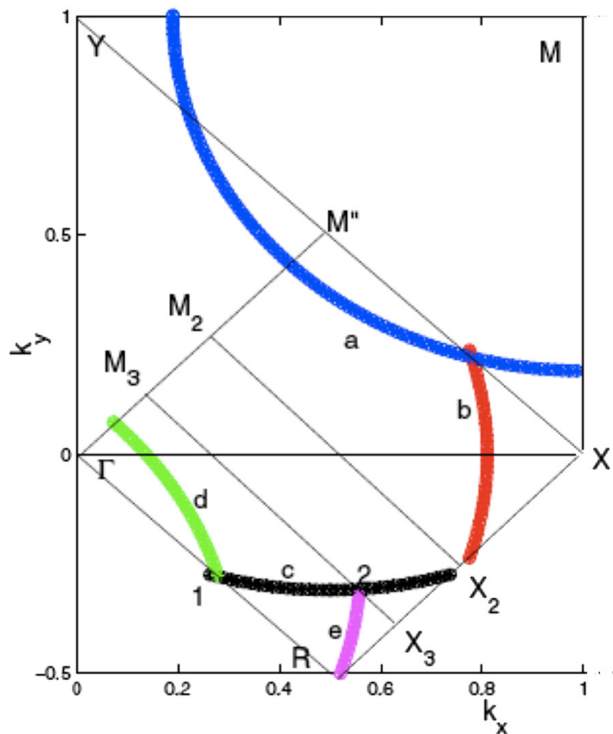


FIG. 6: (Color online) A schematic view of how the circular FS of doped LCO is downfolded into the BZ of the LCO-8 supercell. The BZ for one unit cell is limited by Γ - X - M - Y , and it is downfolded into Γ - R - X_3 - M_3 for the BZ of the supercell.

FS appears to be very distorted compared to the folded FS, and there is no clear separation of states between O_i and the rest of the lattice sites. A similar conclusion about doping can be drawn from the results for doped $\text{La}_2\text{CuO}_{4+\delta}$ (LCO) [23] despite the differences of structure and distribution of O_i . The effective p-doping due to increasing O_i content can be seen from the displacement of the Cu-d band edge, see Fig. 2. The downfolding is shown in Fig. 6 and 7 as for HBCO in Fig. 4, but now the folding is fourfold of the AFM double cell ($\text{La}_4\text{Cu}_2\text{O}_8$) in the diagonal direction.

Three branches (c , d , e) are seen in the folded BZ limited by Γ - R - X_3 - M_3 when the circular FS is downfolded. The top panel of Fig. 7 show the FS of the undoped supercell ($\text{La}_{16}\text{Cu}_8\text{O}_{32}$). The three FS branches from the bands 211-213 agree well with what is expected from the folding. With one O_i ($N=1$), which makes an ordered repetition of quite distant impurities, and thus no "wire", one obtains a quite distorted FS. With two O_i ($N=2$) and a more wire-like order, one retrieves more of the standard FS in the left part of the BZ, but it has moved upwards compared to the case $N=0$, which can be interpreted as coming from a larger radius of the unfolded FS and p-doping. The bands in the right part of the BZ can be traced to the original FS circle, but gaps

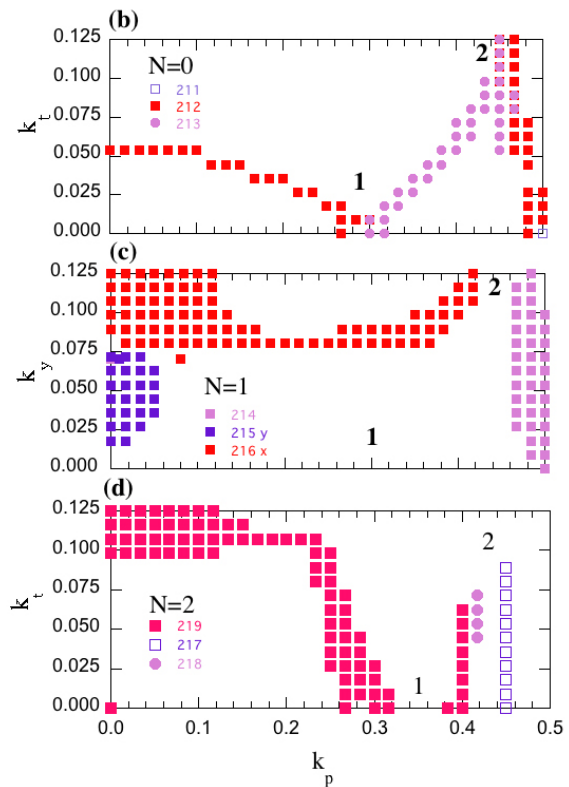


FIG. 7: (Color online) The three panels show the FS for the 3 calculations with no ($N=0$, upper panel), one ($N=1$, middle) and two ($N=2$, lower panel) O_i impurities. As expected, the FS for $N=0$ agree well with the downfolded FS shown in figure 6. With doping, $N=1$ and $N=2$, there is a gradual displacement of the left part of the FS branch, which corresponds to a larger radius of the unfolded FS (near M'), i.e. to a slight p-doping. However, the FS close to the X -point becomes distorted.

have appeared.

The results for $\text{La}_2\text{NiO}_{4+\delta}$ are not easy to interpret. The DOS evolves as in the cuprates, and can be interpreted as a p-doping as O_i are inserted. But the d-band is less filled compared to Cu-d, and the FS is quite complicated already for $N=0$, since E_F falls within the Ni-d bands. The FS for the double cell of undoped $\text{La}_4\text{Ni}_2\text{O}_8$ is shown in Fig. 8. When plotted for the normal simple cell it would have one Γ -centered and another piece centered in the corner of the BZ. These pieces now both appear around the Γ point in Fig. 8. The advantage of displaying the FS of the double cell is that its folding in the diagonal direction (45 degrees with respect to the NiO bonding) easily can be compared to the FS calculated for the $\text{La}_{12}\text{Ni}_6\text{O}_{24}$ supercell, shown in Fig. 9. As for folding in the LCO system, there is a good agreement between folded and calculated FS's. Next, in Fig. 10 we show the calculated FS for $\text{La}_{12}\text{Ni}_6\text{O}_{25}$, i.e. for the case when one O_i atom forms a kind of wire ordering in the supercell. The FS is now quite different from that

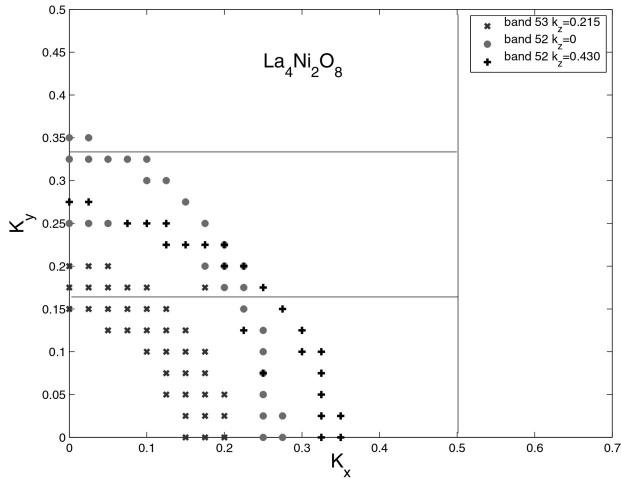


FIG. 8: (Color online) The FS for the double cell $\text{La}_4\text{Ni}_2\text{O}_8$, in which three panels show how the BZ is to be folded to correspond to the BZ for the threefold cell, $\text{La}_{12}\text{Ni}_6\text{O}_{24}$, see Fig. 9.

of the undoped case, and as in the case of O_i -wires in LCO, the FS fragmented in small 'islands'. In contrast to LCO, it is hardly possible to see that the radii of a generic FS-piece have diminished because of an effective doping. The local DOS near and on the O_i wire is not as high as in the LCO system. The hybridization between wire states and the NiO d-p bands is more effective, and the isolation of the wire is not as drastic as in LCO. Nevertheless, a line from a FS structure to the right in Fig. 10 seems to be unexplained from the ordinary bands, and could be due to the isolated O_i band as in doped LCO.

The wire with new potential modulations generates small band gaps within the Ni-O bands. Original bands are cut into smaller 'multi-valley' bands, which for the FS leads to fragmentation. But the interpretation of the FS's for undoped and doped LNO supercell appear not to be as simple as in LCO.

The d-band edge below E_F is displaced with increasing N in a similar manner as in the cuprates, and so the impurities are likely to create an effective p-doping within the NiO layers. An opposite and much stronger "n"-doping would be needed to make the nickelate FS similar to the simple cuprate FS, which naively could be expected to make nickelates superconducting. The calculated FS of the nickelate is not simple and does not resemble the FS of the cuprates, and this is independent of N.

IV. DISCUSSION.

In the three systems we have found evidence of electron charge transfer from the metal-oxide layers to the interstitial O_i impurities. The electron count within the atomic spheres as well as the shift of E_F supports this finding in all cases. When the O_i sites are ordered to form wires in the case of cuprates this p-type charge transfer

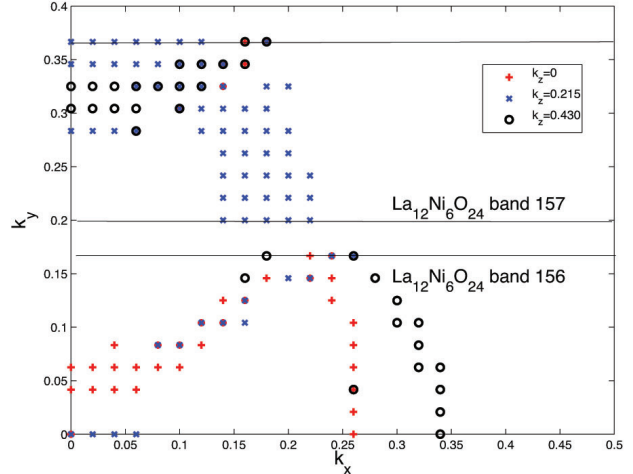


FIG. 9: (Color online) The FS for $\text{La}_{12}\text{Ni}_6\text{O}_{24}$. The FS features can be understood from a folding from the FS shown in Fig. 8.

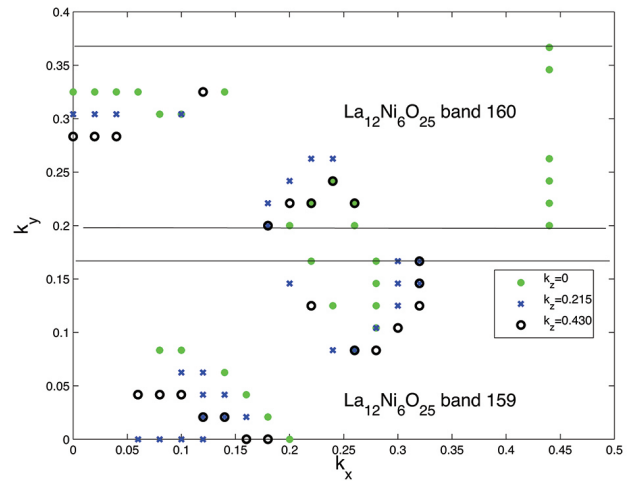


FIG. 10: (Color online) The FS for $\text{La}_{12}\text{Ni}_6\text{O}_{25}$. The addition of the O_i impurity leads to a fragmentation of the FS due to formation of multibands.

has the same effect on the CuO layers as the standard ways of doping, like replacement of La with Sr in LCO. The DOS becomes very high on the O_i wires, but the latter sites are electronically isolated from the CuO layers, and the layers can maintain the generic electronic structure of common cuprates. Without ordering there is more overlap between not too distant O_i sites, and the separation between the electronic structures on CuO layers and O_i is no longer possible. This is at least what we conclude from the absence of a typical CuO layer FS in the case of disordered impurities. It is likely that clustering into "islands" instead of wires also can work for having both the charge transfer and the intact FS property in the layers, but it is not known how far the charge transfer can reach between large well separated islands. Thus,

we suggest that a favorable effect from self-organized O_i wires on T_c can be caused by the doping of the CuO layers, leading to optimal doping with E_F near the van-Hove singularity. But there is a second possibility in the case of wire ordering. Perpendicular periodic wires will set up a new periodicity of the potential, and this is known to make additional band gaps and peaks in the DOS. The strength of the potential modulation and the wavelength determines the energy and the height of peaks and valleys of the DOS. Other types of doping should be able to generate the same modulations, and as has been proposed earlier for phonon and spin waves, an optimization is required to make strong peaks to coincide with E_F and the doping in order to expect an enhancement of T_c [55, 75]. Such a mechanism should help to increase T_c in any system with fairly simple band structures where a periodic potential can make flat bands and higher DOS at precise energies. Here, for cuprates with O_i impurity wires one would expect correlations between impurity concentration (through the distance between wires) and variations of T_c . Unfavorable conditions regarding wire separations and doping could occur and put E_F in a valley of the DOS with low T_c .

Superconducting pairing may depend on phonons, spin fluctuations or even a coupling between the two [75]. Many exchange enhanced systems can be close to either a ferro magnetic (FM) or an anti-ferro magnetic (AFM) transition, and calculations have shown that lattice distortions may trigger the transitions. For instance, FM fluctuations in Ce and B20 type compounds like FeSi are enhanced by thermal lattice disorders [79–82]. AFM fluctuations occur at high pressure in Fe when the lattice transforms from fcc to hcp structure [83, 84], where they probably are important for the occurrence of superconductivity. The onset of FM appears to play a role for anomalous thermal expansion according to calculations for compounds where the total energies are close for the paramagnetic and FM states [85]. Similarly, in highly doped cuprates calculations indicate that a very weak FM state might be preferred over the non-magnetic one [86]. All these examples show that lattice distortions and phonons have an intimate connection with FM, and the calculations with selected vibrational modes indeed enforce spin waves [71, 75]. Here, for wire of O_i in HBCO and LCO it is found that local moments on Cu for imposed AFM waves tend to decrease near the wire (probably due to the hybridization between Cu-d and O-p on O_i) [23, 25]. Further works are needed for telling whether coupling between spin and phonons will be stronger and enhance superconductivity in the systems with O_i wires, or if it will attenuate such couplings near and far from the wires. Ni in undoped LNO show stable FM order [24]. With the large DOS near the O_i wire one could expect enforcement of the local Ni moments near the wire. But the calculation show that the local DOS on Ni near the wire is only about 2/3 of the Ni DOS in undoped LNO and 1/2 of the Ni far from the wire. The FM calculations reflect these DOS variations, since the moment on Ni is

highest far from the wire ($0.25 \mu_B$), lower in pure LNO ($0.18 \mu_B$), while extremely small close to O_i . This shows that the large DOS on (ordered) O_i is very localized to the wire itself (dominated by O-p), but the proximity to the nearest Ni makes an essential non-magnetic layer of Ni. If FM was the only reason for the absence of superconductivity in LNO, then one could hope for pairing within a thin LNO layer near O_i wires. However, as mentioned above, the FS of LNO is very complex and has no resemblance with that of the cuprates, and it is likely that a simple FS is one of the conditions for pairing in the metal-oxide layers.

V. CONCLUSION.

The main conclusion is that interstitial O_i impurities lead to p-doping of the metal-oxide planes in all of the studied systems. Further, ordering of the impurities into wires makes an electronic isolation of the wires and the layers in the cuprates, so that the CuO layers behave much like ordinary p-doped cuprates. The wires of O_i impurities may contribute to a potential modulation with the formation of a new quasi 1D band. The calculated very large DOS peak at E_F is not made from such an effect, but is caused by localized states on the wire. The positive effect on T_c from clustering of O impurities might originate from the hole doping that the excess O's provide to the spacial regions far from the dopants. The latter and the wire regions are spatially and electronically separated, so that superconductivity can take place without negative disturbance from the impurities.

These findings are useful for future experiments, both for spectroscopy and for searching correlation between T_c variations and interstitial doping of oxygen. In fact, theory predicts an oscillatory behavior of DOS height at E_F when impurities cause small periodic perturbations of the potential, but this has not been verified experimentally. Direct measurements of T_c variations in cuprates should constitute a sensitive test of such correlations. The nickelate system has a much more complicated FS and higher metallic DOS near E_F than the cuprates, also after doping. There are no indications that LNO can be doped and develop its band structure into something like that of cuprate superconductors.

In conclusion the present work opens a new scenario for the mechanism of high T_c superconductivity in cuprates. We provide evidence that ubiquitous oxygen wires of finite size, formed in oxygen doped cuprates, give in their proximity, the first set of states with broken Fermi surfaces forming quasi 1D electronic states discussed here and far away from the wires, a second set of states made of a 2D strongly correlated doped Mott insulator. The wires formation gives first quantum confined localized states near the wires which coexist with second delocalized states in the Fermi-surface (FS) of doped cuprates. In the novel scenario for high T_c superconductivity proposed by this work the first set of electronic states is identified as an ar-

ray of Kitaev wires [87] giving Majorana bound states [88] which are proximity-coupled to the second set of states,

far from the oxygen wires, realizing the 2D d-wave superconductor [89, 90]

-
- [1] T. Jarlborg and A. Bianconi, *Scientific Reports* **6**, 24816 (2016)
- [2] A. Bianconi, and T. Jarlborg *Novel Superconducting Materials* **1**, 37 (2015)
- [3] A. Bianconi and T. Jarlborg, *EPL (Europhysics Letters)* **112**, 37001 (2015).
- [4] J. Bardeen, L.N. Cooper and J.R. Schrieffer, *Phys. Rev.* **108**, 1175 (1957).
- [5] Y. Seino, A. Kotani, and A. Bianconi, *Journal of the Physical Society of Japan* **59**, 815 (1990),
- [6] M. Poma, S. Turtu, A. Bianconi, F. Campanella, A. M. Flank, P. Lagarde, C. Li, I. Pettiti, and D. Udron, *Physica C: Superconductivity* **185-189**, 1061 (1991).
- [7] A. Bianconi, S. Agrestini, G. Bianconi, D. Di Castro, and N. L. Saini, *Journal of Alloys and Compounds* **317-318**, 537 (2001).
- [8] S. Agrestini, N. L. Saini, G. Bianconi, and A. Bianconi, *Journal of Physics A: Mathematical and General* **36**, 9133 (2003).
- [9] A. Bianconi, N. L. Saini, T. Rossetti, A. Lanzara, A. Perali, M. Missori, H. Oyanagi, H. Yamaguchi, Y. Nishihara, and D. H. Ha, *Phys. Rev. B* **54**, 12018 (1996).
- [10] G. Campi, A. Bianconi, N. Poccia, G. Bianconi, L. Barba, G. Arrighetti, D. Innocenti, J. Karpinski, N. D. Zhigadlo, S. M. Kazakov, et al., *Nature* **525**, 359 (2015).
- [11] G. Campi, A. Ricci, N. Poccia, L. Barba, G. Arrighetti, M. Burghammer, A. S. Caporale, and A. Bianconi, *Phys. Rev. B* **87**, 014517 (2013).
- [12] G. Campi and A. Bianconi, *Journal of Superconductivity and Novel Magnetism* **29**, 627 (2016).
- [13] G. Bianconi, *Multilayer networks : structure and function*, Oxford University Press, Oxford, United Kingdom (2018). isbn: 9780198753919
- [14] A. Bianconi, *Solid State Communications* **91**, 1 (1994).
- [15] A. Bianconi, *Journal of Superconductivity* **18**, 625 (2005),
- [16] A. Perali, A. Bianconi, A. Lanzara, and N. L. Saini, *Solid State Communications* **100**, 181 (1996),
- [17] A. Valletta, A. Bianconi, A. Perali, and N. L. Saini, *Zeitschrift fur Physik B Condensed Matter* **104**, 707 (1997).
- [18] L. Simonelli, M. Fratini, V. Palmisano, M. Filippi, N. Saini, and A. Bianconi, *Journal of Superconductivity and Novel Magnetism* **18**, 773 (2005).
- [19] A. Bianconi, *Journal of Physics and Chemistry of Solids* **67**, 567 (2006).
- [20] M. Fratini, N. Poccia, A. Ricci, G. Campi, M. Burghammer, G. Aeppli and A. Bianconi, *Nature* **466**, 841 (2010).
- [21] N. Poccia, M. Fratini, A. Ricci, G. Campi, L. Barba, A. Vittorini-Orgeas, G. Bianconi, G. Aeppli, A. Bianconi, *Nature Materials*, **10**, 733 (2011).
- [22] P. Littlewood, *Nature Materials*, **10**, 726 (2011).
- [23] T. Jarlborg and A. Bianconi, *Phys. Rev. B* **87**, 054514 (2013).
- [24] T. Jarlborg, and A. Bianconi, *J. Supercond. Nov. Magn.* **29**, 615 (2016)
- [25] T. Jarlborg and A. Bianconi, *J. Supercond. Nov. Magn.* **31**, 689 (2018).
- [26] A. Bianconi and M. Missori, in *Phase separation in cuprate superconductors*, edited by: E. Sigmund, K. A. Muller (Springer-Verlag, 1994).
- [27] D. Di Castro, G. Bianconi, M. Colapietro, A. Pifferi, N. L. Saini, S. Agrestini, and A. Bianconi, *The European Physical Journal B - Condensed Matter and Complex Systems* **18**, 617 (2000),
- [28] F. V. Kusmartsev, D. Di Castro, G. Bianconi, and A. Bianconi, *Physics Letters A* **275**, 118 (2000),
- [29] P. Barnes, M. Avdeev, J. Jorgensen, D. Hinks, H. Claus, and S. Short, *Phys. Rev. B* **72**, 134515 (2005).
- [30] T. H. Geballe and M. Marezio, *Physica C* **469**, 680 (2009).
- [31] W. B. Gao, Q. Q. Liu, L. X. Yang, Y. Yu, F. Y. Li, C. Q. Jin and S. Uchida, *Phys. Rev. B* **80**, 094523 (2009).
- [32] O. Chmaissem, I. Grigoraviciute, H. Yamauchi, M. Karppinen, and M. Marezio, *Phys. Rev. B* **82**, 104507 (2010).
- [33] M. Marezio, O. Chmaissem, C. Bougerol, M. Karppinen, H. Yamauchi, and T. H. Geballe, *APL Materials* **1**, 021103 (2013)
- [34] P. Giraldo-Gallo, et al., *Nature Communications* **6**, 8231 (2015).
- [35] A. Ricci, N. Poccia, G. Campi, B. Joseph, G. Arrighetti, L. Barba, M. Reynolds, M. Burghammer, H. Takeya, Y. Mizuguchi, Y. Takano, M. Colapietro, N. Saini, A. Bianconi *Phys. Rev. B* **84**, 060511, (2011).
- [36] A. Ricci, N. Poccia, B. Joseph, G. Arrighetti, L. Barba, J. Plaisier, G. Campi, Y. Mizuguchi, H. Takeya, Y. Takano, et al., *Superconductor Science and Technology* **24**, 082002 (2011)
- [37] A. Ricci et al. *Scientific Reports* **3**, 2383 (2013)
- [38] A. Ricci, N. Poccia, G. Campi, F. Coneri, L. Barba, G. Arrighetti, M. Polentarutti, M. Burghammer, M. Sprung, M.v Zimmermann and A. Bianconi, *New Journal of Physics* **16**, 053030 (2014). .
- [39] G. Campi, A. Ricci, N. Poccia, A. Bianconi, *Journal of Superconductivity and Novel Magnetism* **27**, 987 (2014).
- [40] I. Zeljkovic, et al. *Nature Materials* **11**, 585 (2012).
- [41] I. Zeljkovic and J. E. Hoffman, *Physical Chemistry Chemical Physics* **15**, 13462 (2013),
- [42] I. Zeljkovic, et al., *Nano Lett.* **14**, 6749 (2014).
- [43] A. Bianconi, *International Journal of Modern Physics B* **14**, 3289 (2000).
- [44] V. Kresin, Y. Ovchinnikov and S. Wolf, *Physics Reports* **431**, 231 (2006).
- [45] G. Bianconi, *Physical Review E* **85**, 061113 (2012);
- [46] G. Bianconi, *Journal of Statistical Mechanics: Theory and Experiment* **2012**, P07021 (2012).
- [47] G. Bianconi, *Europhysics Letters* **101**, 26003 (2013).
- [48] K. I. Kugel, A. L. Rakhmanov, A. O. Sboychakov, N. Poccia, and A. Bianconi, *Phys. Rev. B.* **78**, 165124 (2008).
- [49] K.I. Kugel, A.L. Rakhmanov, A.O. Sboychakov, F.V. Kusmartsev, N.Poccia, and A.Bianconi, *Superconductor Science and Technology* **22**, 014007 (2009)
- [50] A. Bianconi, N. Poccia, A. O. Sboychakov, A. L.

- Rakhmanov, and K.I. Kugel, *Superconductor Science and Technology* **28**, 024005 (2015)
- [51] A. Bianconi, *Quantum Materials: Shape Resonances in Superstripes*, *Nature Physics* **9**, 536 (2013).
- [52] M. Fratini, N. Poccia and A. Bianconi *Journal of Physics: Conference Series* **108**,1012036 (2008)
- [53] A. Bianconi *Journal of Superconductivity* **18**, 625 (2005).
- [54] A. Bianconi, S. Agrestini, G. Campi, M. Filippi, and N. L. Saini, *Current Applied Physics* **5**, 254 (2005),
- [55] T. Jarlborg, *Appl. Phys. Lett.* **94**, 212503, (2009).
- [56] T. Jarlborg, B. Barbiellini, R. S. Markiewicz and A. Bansil, *Phys. Rev. B* **86**, 235111 (2012)
- [57] T. Jarlborg, A. Bianconi, B. Barbiellini, R. S. Markiewicz, and A. Bansil, *J. Supercond. Nov. Magn.* **26**, 2597 (2013),
- [58] T. Jarlborg, *Phys. Rev. B* **68**, 172501 (2003).
- [59] T. Jarlborg and G. Santi, *Physica C* **329**, 243 (2000).
- [60] T. Jarlborg, *Phys. Rev. B* **84**, 064506 (2011).
- [61] Z.Wu, N.Saini, and A.Bianconi, *Physical Review B* **64**, 092507 (2001)
- [62] A.Lanzara, N.L. Saini, A.Bianconi, F.Duc, and P.Bordet, *Physical Review B* **59**, 3851 (1999)
- [63] P. Bordet, F.Duc, P.G. Radaelli, A.Lanzara, N.Saini, A.Bianconi, and E.V. Antipov, *Physica C: Superconductivity* **282-287**, 1081 (1997),
- [64] A. Bianconi, S.Doniach, and D.Lublin, *Chemical Physics Letters* **59**, 121 (1978)
- [65] J. Garcia, A. Bianconi, M. Benfatto, and C. R. Natoli, *Le Journal de Physique Colloques* **47** C8-49 (1986).
- [66] O. K. Andersen, *Phys. Rev. B* **12**, 3060 (1975).
- [67] B. Barbiellini, S. B. Dugdale and T. Jarlborg, *Comput. Mater. Sci.* **28**, 287 (2003).
- [68] W. Kohn and L.J. Sham, *Phys. Rev.* **140**, A1133 (1965)
- [69] O. Gunnarsson and B.I. Lundquist, *Phys. Rev. B* **13**, 4274 (1976).
- [70] B. Barbiellini and T. Jarlborg, *Phys. Rev. B* **50**, 3239 (1994).
- [71] T. Jarlborg, *Phys. Rev. B* **64**, 060507(R), (2001).
- [72] W. E. Pickett, *Rev. Mod. Phys.* **61**, 433 (1989).
- [73] A. Damascelli, Z.-X. Shen and Z. Hussain, *Rev. Mod. Phys.* **75**, 473, (2003).
- [74] B. Barbiellini, P. Genoud, J.Y. Henry, L. Hoffmann, T. Jarlborg, A.A. Manuel, S. Massidda, M. Peter, W. Sadowski, H.J. Scheel, A. Shukla, A.K. Singh and E. Walker, *Phys. Rev. B* **43**, 7810 (1991).
- [75] T. Jarlborg, *Physica C* **454**, 5, (2007).
- [76] T. Jarlborg, *Phys. Rev. B* **76**, 140504(R), (2007).
- [77] T. Jarlborg, *J. of Supercond. and Novel Magn.*, **28**, 1231 (2014)
- [78] P. Lazić, D. Pelc, M. Požek, V. Despoja, and D.K. Sunko, *J. of Supercond. and Novel Magn.* **28**, 1299, (2014)
- [79] T. Jarlborg, *Phys. Rev. B* **89**, 184426, (2014).
- [80] T. Jarlborg, *Phys. Rev. B* **55**, 1288, (1997).
- [81] T. Jarlborg, *Phys. Rev. B* **59**, 15002 (1999).
- [82] T. Jarlborg, *Phys. Lett. A* **236**, 143, (1997).
- [83] T. Jarlborg, *Physica C* **385**, 513, (2003).
- [84] T. Jarlborg, *Phys. Lett. A* **300**, 518, (2003).
- [85] E. G. Moroni and T. Jarlborg, *Phys. Rev. B* **41**, 9600, (1990).
- [86] B. Barbiellini and T. Jarlborg, *Phys. Rev. Lett.* **101**, 157002, (2008).
- [87] A . Y. Kitaev *Phys. Usp.* **44**,131, (2001).
- [88] R. M. Lutchyn, J. D. Sau and S. Das Sarma *Phys. Rev. Lett.* **105**, 077001 (2010).
- [89] C. W. J. Beenakker *Annu. Rev. Con. Mat. Phys.* **4**, 113 (2013).
- [90] P. Zhang and F. Nori, *New Journal of Physics* **18**, 043033 (2016).